

Camera Parameters Estimation from Hand-labelled Sun Sositions in Image Sequences

Jean-François Lalonde, Srinivasa G. Narasimhan and Alexei A. Efros
`{jllalonde,srinivas,efros}@cs.cmu.edu`

CMU-RI-TR-08-32

July 2008

The Robotics Institute
Carnegie Mellon University
Pittsburgh, Pennsylvania 15213

© Carnegie Mellon University

Abstract

We present a novel technique to determine camera parameters when the sun is visible in an image sequence. The technique requires a user to label the position of the sun in a few images. We show that it can be used to successfully recover the camera focal length, as well as its azimuth and zenith angles. The method is thoroughly evaluated on synthetic data under a wide range of operating conditions, and representative examples are shown on real data. Ground truth parameters can be recovered with less than 3% error in challenging cases.

Contents

1	Introduction	1
1.1	Assumptions	1
1.2	Related Work	1
2	Geometry of the Problem	2
3	Determining the Camera Parameters	3
4	Validation on Synthetic Data	4
4.1	Focal Length	5
4.2	Camera Zenith	5
4.3	Camera Azimuth	6
5	Representative Results on Real Data	7
6	Summary	8

1 Introduction

In this document, we show that if the sun is visible in a few frames of an outdoor webcam sequence, we can use its position to recover three important camera parameters: its focal length, and its azimuth and zenith angles. This method was used in [5] to evaluate the quality of their sky-based algorithm.

The rest of the document is divided as follows. First, we introduce the few assumptions that need to be made in order for this method to work, followed by a brief presentation of related work. We then illustrate the problem geometry in Sect. 2, and show a method that recovers the camera parameters in Sect. 3. Finally, we demonstrate the performance of our algorithm on synthetic (Sect. 4) and real (Sect. 5) data.

1.1 Assumptions

In order to simplify the problem, we start by making a few realistic assumptions about the camera. First, the camera GPS location is assumed to be known, and all the images must be time-tagged. We also assume the camera has square pixels, and that it has no roll angle, so we need only estimate the yaw and pitch angles. This corresponds to the typical situation where the camera is looking “straight”. Of course, the sun has to be visible in a few frames, and we will assume its position has been hand-labeled by an expert.

1.2 Related Work

Camera calibration has been extensively studied in the computer vision community. Most available methods require the use of a physical calibration target that must be placed within the camera field of view [8, 2]. However, these methods cannot be used if the camera is not physically accessible.

In the case of a static camera acquiring a time-tagged sequence of images, it is possible to use natural features such as the sun and sky to estimate some camera parameters. Cozman and Krotkov [1] proposed to use the sun altitude to recover the camera geolocation (latitude and longitude). Their method is very accurate, but relies on precise measurements using a high-quality camera and inclinometer. Trebi-Ollenu et al. [7] proposed a way to determine the camera heading (i.e. camera azimuth) by detecting the sun using a custom-designed sun sensor. In our case, we do not have access to any additional hardware to ensure precise sun detection in images, so we rely on a user to indicate the sun position in a few images.

Of particular relevance to our work, Jacobs et al. [3] show how they can reliably geolocate the camera by correlating the intensity variations in the images with satellite imagery. Since our approach requires a priori knowledge of the camera position, this technique could be used to initialize our approach, thus enabling the recovery of position and orientation automatically.

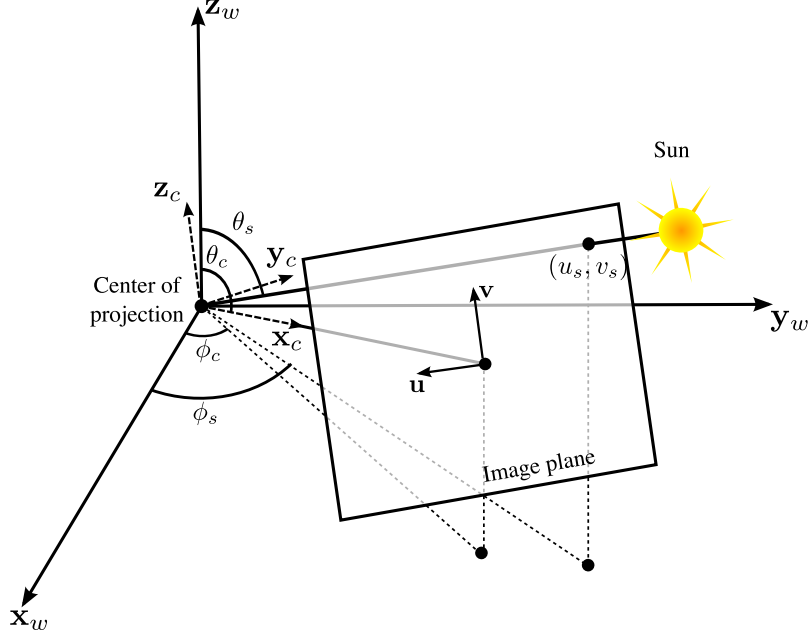


Figure 1: Geometry of the problem.

2 Geometry of the Problem

Let us first start by illustrating the geometry of the problem and introduce corresponding symbols, which will be used throughout this paper. Consider Fig. 1, where a camera with reference frame $(\mathbf{x}_c, \mathbf{y}_c, \mathbf{z}_c)$ is looking at a scene, and the sun is projected at pixels (u_s, v_s) in the image. Our goal is to recover camera parameters from multiple images where the sun is visible, at different (u_s, v_s) coordinates.

If the center of projection of the camera coincides with the origin of the world reference frame $(\mathbf{x}_w, \mathbf{y}_w, \mathbf{z}_w)$ and that its optical axis is aligned with the positive \mathbf{x}_w -axis, we need only estimate the camera orientation, θ_c and ϕ_c , as well as its focal length f_c . The sun angular position (θ_s, ϕ_s) can be computed for a given image from its GPS location and time of capture using the method of Reda and Andreas [6].

To compute the projection of the sun in the image, we first compute the 3-D vector associated to the sun:

$$\mathbf{s} = \begin{bmatrix} x_s \\ y_s \\ z_s \end{bmatrix} = \begin{bmatrix} \sin \theta_s \cos \phi_s \\ \sin \theta_s \sin \phi_s \\ \cos \theta_s \end{bmatrix}. \quad (1)$$

We can express the sun 3-D coordinates in the camera local coordinate system,

by rotating \mathbf{s} according to (θ_c, ϕ_c) :

$$\mathbf{s}' = R^{-1}\mathbf{s}, \quad (2)$$

where

$$R = R_1 R_2 = \begin{bmatrix} \cos \phi_c & -\sin \phi_c & 0 \\ \sin \phi_c & \cos \phi_c & 0 \\ 0 & 0 & 1 \end{bmatrix} \begin{bmatrix} \cos(\pi/2 - \theta_c) & 0 & \sin(\pi/2 - \theta_c) \\ 0 & 1 & 0 \\ -\sin(\pi/2 - \theta_c) & 0 & \cos(\pi/2 - \theta_c) \end{bmatrix}. \quad (3)$$

By properties of rotation matrices, we can express R^{-1} directly:

$$\begin{aligned} R^{-1} &= (R_1 R_2)^{-1} = R_2^{-1} R_1^{-1} = R_2^T R_1^T \\ &= \begin{bmatrix} \cos(\pi/2 - \theta_c) & 0 & -\sin(\pi/2 - \theta_c) \\ 0 & 1 & 0 \\ \sin(\pi/2 - \theta_c) & 0 & \cos(\pi/2 - \theta_c) \end{bmatrix} \begin{bmatrix} \cos \phi_c & \sin \phi_c & 0 \\ -\sin \phi_c & \cos \phi_c & 0 \\ 0 & 0 & 1 \end{bmatrix} \\ &= \begin{bmatrix} \sin \theta_c \cos \phi_c & \sin \theta_c \sin \phi_c & -\cos \theta_c \\ -\sin \phi_c & \cos \phi_c & 0 \\ \cos \theta_c \cos \phi_c & \cos \theta_c \sin \phi_c & \sin \theta_c \end{bmatrix}. \end{aligned} \quad (4)$$

We then project the sun position in the image by re-arranging the axes such that the projection axes (u, v) point in the direction corresponding to the drawing in Fig. 1:

$$u_s = \frac{-f_c y'_s}{x'_s} \quad v_s = \frac{f_c z'_s}{x'_s}. \quad (5)$$

3 Determining the Camera Parameters

Given the geometry of the problem presented in the previous section, we now propose a way to use the sun positions to determine the focal length, zenith and azimuth angles of a camera. The idea is to minimize the reprojection error, that is, minimize the distance between the sun labels and the sun position projected onto the image plane. If we have several observations, we can find the solution that best fits the data in a least-squares sense:

$$\min_{f_c, \theta_c, \phi_c} \sum_{i=1}^N \|\mathbf{p}_i - \mathcal{P}(R^{-1}\mathbf{s}_i)\|^2, \quad (6)$$

where $\mathbf{p}_i = [u_i \ v_i]^T$ are the sun labels in the image plane, and \mathcal{P} is the projection operator (5). Our goal is to find the camera parameters (f_c, θ_c, ϕ_c) that will best align the sun labels \mathbf{p}_i with the rotated sun position \mathbf{s}'_i projected in the image. Written explicitly, we minimize:

$$\min_{f_c, \theta_c, \phi_c} \sum_{i=1}^N \left(u_i - \frac{-f_c y'_{s,i}}{x'_{s,i}} \right)^2 + \left(v_i - \frac{f_c z'_{s,i}}{x'_{s,i}} \right)^2, \quad (7)$$

Name	Symbol	Default value
Focal length	f_c	1000 px
Number of image	N	20
Camera zenith	θ_c	90°
Camera azimuth	ϕ_c	0° (North)

Table 1: Default values for each parameters used in the experiments on synthetic data. Symbols for each parameter are also shown, “_” is used when the symbol is not referred to in any equation.

where $(x'_{s,i}, y'_{s,i}, z'_{s,i})$ are defined by

$$\begin{aligned}
 x'_{s,i} &= \sin \theta_c \cos \phi_c x_{s,i} + \sin \theta_c \sin \phi_c y_{s,i} + \cos \theta_c z_{s,i} \\
 y'_{s,i} &= -\sin \phi_c x_{s,i} + \cos \phi_c y_{s,i} \\
 z'_{s,i} &= -\cos \theta_c \cos \phi_c x_{s,i} - \cos \theta_c \sin \phi_c y_{s,i} + \sin \theta_c z_{s,i}
 \end{aligned} \tag{8}$$

Equation (7) is a non-linear least-squares minimization in the parameters (θ_c, ϕ_c) , which can be solved using Levenberg-Marquadt. The procedure is initialized by finding the minimum value for (7) over a discretized grid in the parameter space.

4 Validation on Synthetic Data

In order to thoroughly validate our approach, we test it under a very wide variety of conditions using synthetically-generated data. Data points are generated randomly from a uniform distribution within the visible sky area (above the horizon line).

We evaluate the influence of four parameters:

- The camera focal length f_c .
- The number of available images N . In practice, the sun might not be visible in many images.
- The camera zenith angle θ_c . This angle indicates whether the camera is pointing up or down.
- The camera azimuth angle ϕ_c . This is the angle of the camera with respect to North (increasing towards West).

Gaussian noise in labeling precision is also added in order to evaluate its influence on the quality of the results. In order to account for the randomness in point selection, we perform each experiment 20 times, and show the corresponding error bars.

For each plot shown below, one parameter is varied at a time, and the others are kept constant at a default value. Table 1 indicates the default values for each parameter. In addition, only results obtained by minimizing the 3-D distance are shown, because those obtained by minimizing the reprojection error are very similar.

4.1 Focal Length

The plots illustrating the error in focal length estimation are shown in Fig. 2. In the noisy case, the estimation error is at most 1.5%, when the input focal length is very small (see Fig. 2-(a)). Estimation quality does not seem to be affected by the horizon line position or the camera azimuth, as shown in Fig. 2-(c) and (d).

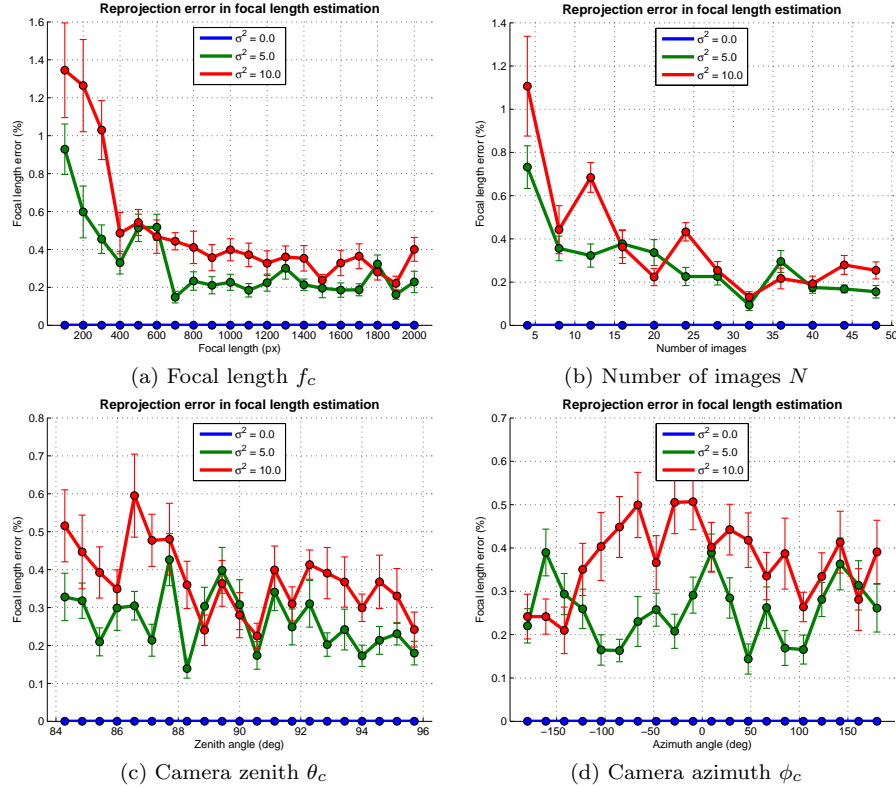


Figure 2: Error in focal length estimation as a function of several parameters, and noise level. For each plot, one parameter is varied, while the others are kept fixed at their default values. The default values used in all the experiments are shown in Table 1. Three different gaussian noise levels are shown, ranging from no noise ($\sigma^2 = 0$), low ($\sigma^2 = 5$) and high ($\sigma^2 = 10$).

4.2 Camera Zenith

The plots illustrating the error in camera zenith estimation are shown in Fig. 3. The results are very similar to the ones obtained for the focal length. In the noisy case, the estimation error is at most 0.5° , when the input focal length is

very small (see Fig. 3-(a)). Estimation quality does not seem to be affected by the horizon line position or the camera azimuth, as shown in Fig. 3-(c) and (d).

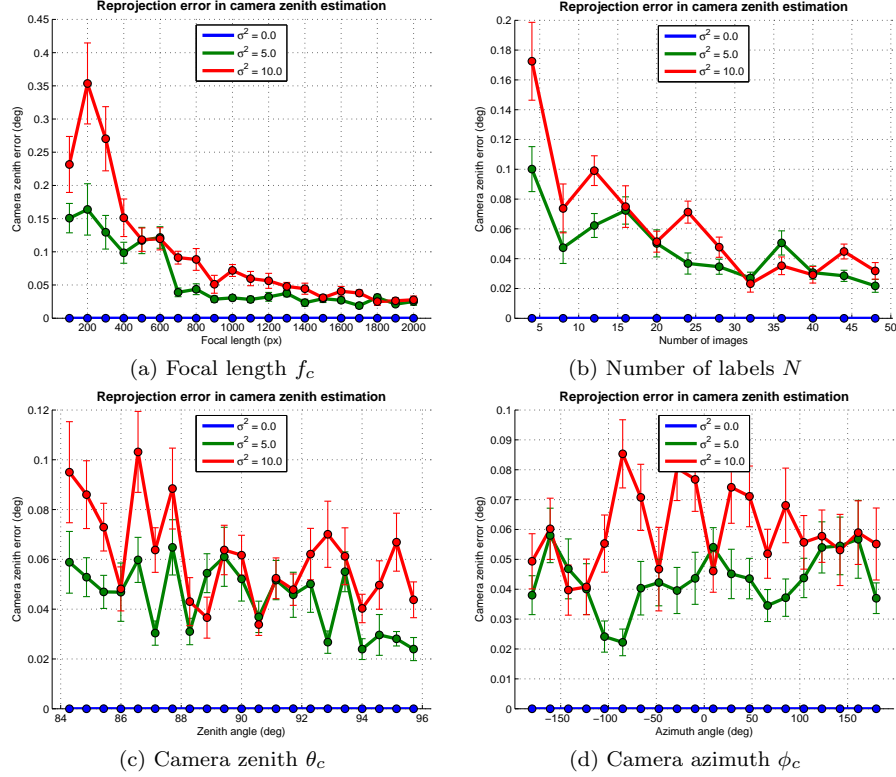


Figure 3: Error in camera zenith estimation as a function of several parameters, and noise level. For each plot, one parameter is varied, while the others are kept fixed at their default values. The default values used in all the experiments are shown in Table 1. Three different gaussian noise levels are shown, ranging from no noise ($\sigma^2 = 0$), low ($\sigma^2 = 5$) and high ($\sigma^2 = 10$).

4.3 Camera Azimuth

The plots illustrating the error in camera azimuth estimation are also very similar to the previous ones, and are shown in Fig. 4. In the noisy case, the estimation error is at most 0.4° , when the input focal length is very small (see Fig. 4-(a)). Estimation quality does not seem to be affected by the horizon line position or the camera azimuth, as shown in Fig. 4-(c) and (d).

Using synthetic data, we were able to demonstrate the usefulness of our approach in a very wide variety of situations. However, we also need to test it using real data to show its usefulness in real applications.

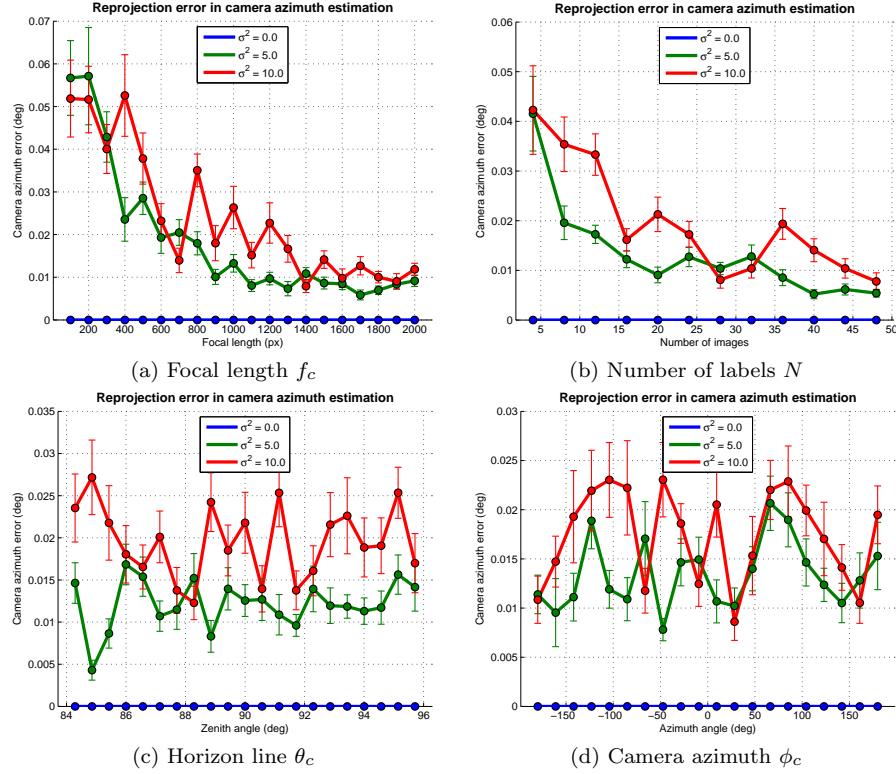


Figure 4: Error in camera azimuth estimation as a function of several parameters, and noise level. For each plot, one parameter is varied, while the others are kept fixed at their default values. The default values used in all the experiments are shown in Table 1. Three different gaussian noise levels are shown, ranging from no noise ($\sigma^2 = 0$), low ($\sigma^2 = 5$) and high ($\sigma^2 = 10$).

5 Representative Results on Real Data

When the sun is visible in an image sequence, it is possible to recover the camera parameters using the technique presented in this document. To validate the results, we can then predict the sun position in all the images, even those that have not been labeled, and inspect the results visually. Fig. 5 shows a few examples of predicted sun positions for a typical image sequence. The horizon line can also be predicted from the recovered camera parameters as an additional way of evaluating the quality of the results:

$$v_h = -f_c \tan(\pi/2 - \theta_c). \quad (9)$$

Table 2 shows the estimated parameters for the same sequence.

f_c	651.57 px
ϕ_c	93.39° West
θ_c	85.94°

Table 2: Summary of the estimated values for the sequence shown in Fig. 5.

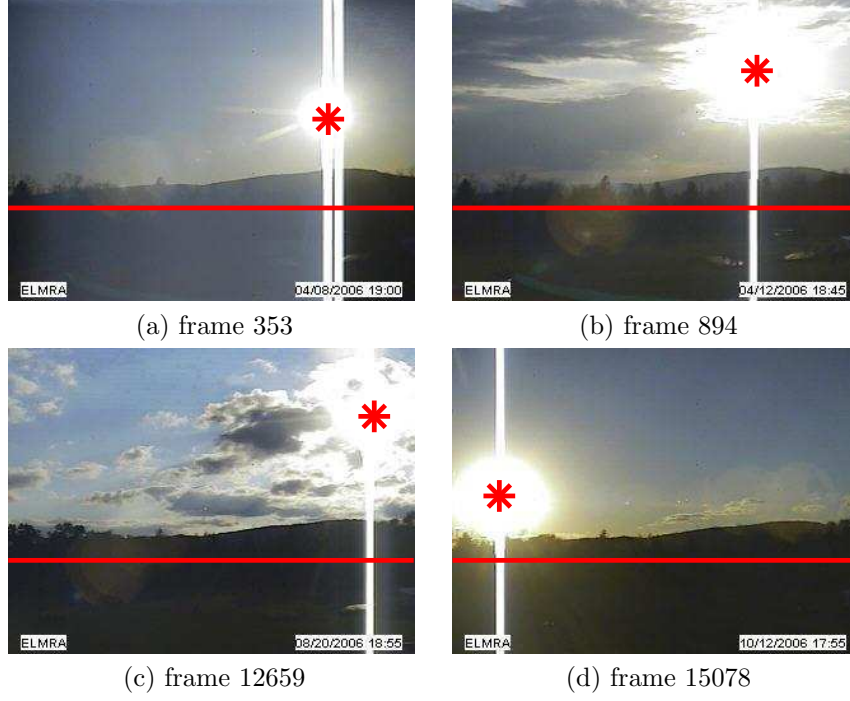


Figure 5: Sun position and horizon prediction. The sun position (yellow star) and horizon line (red horizontal line) is predicted for un-labelled images from a typical sequence where the sun is visible. Note that the first and second row of images are separated by 4 months, but the accuracy is not affected. The horizon line is never explicitly labelled, but can still be successfully recovered.

6 Summary

We presented a technique to determine the camera parameters when the sun is visible in an image sequence. The technique requires a user to label the position of the sun in a few images. In particular, this technique is used in [5] to obtain high precision estimates of the camera parameters and thus serve as a basis for evaluating their calibration-from-sky algorithm.

References

- [1] F. Cozman and E. Krotkov. Robot localization using a computer vision sextant. In *IEEE International Conference on Robotics and Automation*, 1995.
- [2] J. Heikkilä. Geometric camera calibration using circular control points. *IEEE Transactions on Pattern Analysis and Machine Intelligence*, 22(10):1066–1077, October 2000.
- [3] N. Jacobs, S. Satkin, N. Roman, R. Speyer, and R. Pless. Geolocating static cameras. In *IEEE International Conference on Computer Vision*, 2007.
- [4] K. Kanatani. Analysis of 3-D rotation fitting. *IEEE Transactions on Pattern Analysis and Machine Intelligence*, 16(5):543–549, May 1994.
- [5] J.-F. Lalonde, S. G. Narasimhan, and A. A. Efros. What does the sky tell us about the camera? In *European Conference on Computer Vision*, 2008.
- [6] I. Reda and A. Andreas. Solar position algorithm for solar radiation applications. Technical Report NREL/TP-560-34302, National Renewable Energy Laboratory, November 2005.
- [7] A. Trebi-Ollennu, T. Huntsberger, Y. Cheng, E. T. Baumgartner, B. Kennedy, and P. Schenker. Design and analysis of a sun sensor for planetary rover absolute heading detection. *IEEE Transactions on Robotics and Automation*, 17(6):939–947, December 2001.
- [8] Z. Zhang. A flexible new technique for camera calibration. *IEEE Transactions on Pattern Analysis and Machine Intelligence*, 22(11):1330–1334, 2000.